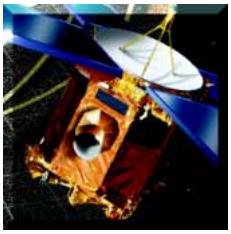

The Near-Infrared Spectrometer

Keith Peacock, Jeffery W. Warren, and Edward H. Darlington

The Near-Infrared Spectrometer (NIS) instrument will map the spectral properties of asteroid 433 Eros in the range 800–2600 nm to determine its mineral content. Optically, NIS uses a scan mirror and an imaging mirror to project an image at a field stop. A grating spectrometer disperses the energy, and a dichroic beamsplitter separates two spectral orders, reflecting the short wavelengths, 816–1500 nm, to a 32-element Ge detector, and transmitting the long wavelengths, 1500–2600 nm, to a 32-element InGaAs detector. The spectral resolutions are 22 and 44 nm for the second and first spectral orders, respectively. A scan mirror rotates the field of view over a 140° range that includes a solar-illuminated calibration target. Spectra are measured once per second using a selection of data acquisition macros. The properties of the instrument were extensively measured during on-ground calibration, and in-flight calibration was begun shortly after launch. The NIS will observe Eros during approach to the asteroid and will produce composition maps of the entire illuminated surface at spatial resolutions as high as ≈300 m.
(Keywords: Asteroids, NEAR spacecraft, Space instrumentation, Space optics, Spectrographs.)

DESIGN OBJECTIVES AND REQUIREMENTS

An important scientific objective of the Near Earth Asteriod Rendezvous (NEAR) mission is the measurement of the elemental and mineralogic composition of the surface of asteroid 433 Eros with sufficient accuracy to enable comparisons with major meteorite types. To accomplish this, APL developed the Near-Infrared Spectrometer (NIS) to measure the spectrum of sunlight reflected from the surface of Eros in the 800–2600 nm wavelength range. Reflectance spectroscopy has proved to be a powerful tool for the remote mineralogic characterization of planetary and asteroidal surfaces from both ground-based and spacecraft platforms, because many common rock-forming minerals have diagnostic absorption features at visible and near-infrared wavelengths. A high signal-to-noise ratio (SNR) is required to discriminate the subtle compositional/mineralogic differences, and high spatial-resolution global coverage is needed to measure spatial variations in surface properties. The low orbital velocity of the NEAR spacecraft relative to the asteroid allows significant integration times for high SNR. To use the high SNR data effectively, the responsivity of the instrument

as a function of wavelength and its radiometric response were well characterized in a comprehensive prelaunch calibration effort. Because the instrument is operating with DC signals at very low levels, an in-flight optical calibration capability was provided to correct for channel-to-channel drifts in radiometric calibration over 3 years in flight.

The NEAR spacecraft concept calls for all instruments to be body-fixed and to operate in the vicinity of 90° phase angle (near the dawn–dusk terminator), which is the typical viewing geometry of Eros during the orbital phase of the mission. Because the higher illumination and lack of shadows near zero phase angle are critical to reflectance spectroscopy, the NIS includes a scanning capability to observe the asteroid at zero phase during the initial flyby and possibly during the plane flip maneuver later in the mission. The NIS is the only NEAR instrument with this capability.

INSTRUMENT DESIGN

Overview

Because of the limited development time imposed by the tight NEAR schedule, the NIS design is a modification of one used for the Special Sensor Ultraviolet Spectrographic Imager intended to fly on the Defense Meteorological Satellite. The modifications included a different grating to change the wavelength range, use of a dichroic filter to separate the first and second spectral orders, a reduction in the field of view (FOV) by use of a shorter slit, and replacement of the imaging detectors with linear array detectors. Use of an existing mechanical design did not compromise the scientific capability of the instrument. Rather, the design provided the key to rapid development at low cost.

Figures 1a and 1b are photographs of the NIS and associated components taken during final instrument-level testing. The labels show the optics housing, the germanium (Ge) and indium gallium arsenide (InGaAs) detector modules, which are bolted to the housing, the spacecraft mounting bracket that mounts the NIS to the spacecraft at the appropriate angle, the support electronics, and the data processing unit (DPU). In the photograph, the intra-instrument harness is in place, and the heaters and thermostats have been installed, but no thermal blanketing is in place. Also, the cover on the front of the instrument is closed. APL designed the optics of the NIS, and SSG, Inc., of Waltham, Massachusetts, subcontracted to APL for the manufacture of the optics and housing.

APL designed and built the two detectors and their electronics, which are located in separate housings that bolt onto the optics housing. Each detector is a linear array of 32 elements. The detectors and their associated electronics are passively cooled to around –35°C. The detector data are digitized within the detector housings and communicated digitally to the DPU.

(a)

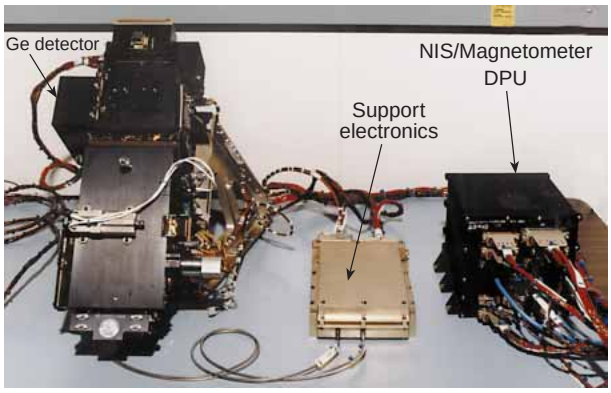

(b)

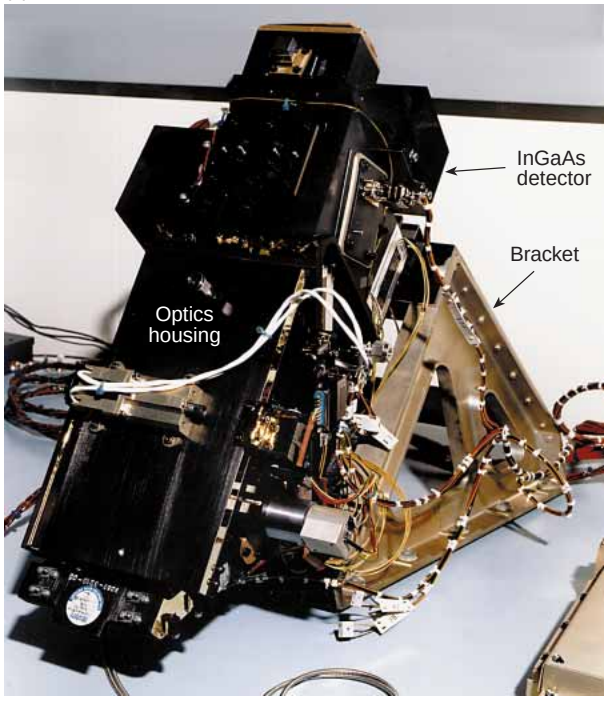

Figure 1. Photographs of the NIS taken during integration and testing. (a) The complete system including the NIS, the support electronics, and the data processing unit. During the flyby, the direction to the asteroid would be overhead in this photograph, and during orbital operations, it would be approximately toward the camera. (b) The NIS instrument is shown mounted on the bracket that positions it on the spacecraft. Thermal blankets are not in place in this photograph. Relative to the instrument, the nominal direction to the Sun when the instrument is mounted on the spacecraft would be into the floor.

Table 1 lists key specifications of the instrument. The table shows the spectral range of the NIS as 800 to approximately 2600 nm. Although the instrument covers the spectral range out to 2700 nm, the useful SNR only extends to about 2600 nm because the detector response is close to the cutoff.

The wide field of regard allows the NIS to operate during different phases of the mission. During orbital

Table 1. Near-Infrared Spectrometer specifications.

Characteristic	Design value
Spectral range	
First order (InGaAs detector)	1400 to ≈2600 nm
Second order (Ge detector)	800 to 1500 nm
Spectral resolution with narrow slit	
First order	44 nm
Second order	22 nm
Field of view	
Narrow slit	0.38 × 0.76°
Wide slit	0.76 × 0.76°
Field of regard	140°
Scan step size	0.4°
Collecting area	5 cm^2
Detector array size	1 × 16 mm
Number of elements per array	32
Size of detector elements	1 × 0.5 mm
Mass	14.03 kg

operations around Eros, the line of sight will be approximately out the "side" of the spacecraft, near the line of sight of the imager and other instruments. During the flyby phase, the spacecraft will pass between the asteroid and the Sun at low speed (5 m/s nominally) to measure the gravitational deflection and also to permit NIS data to be acquired at low phase angle. This acquisition of data requires the line of sight to be shifted approximately 90° to the anti-Sun direction from the instrument nadir. The asteroid will subtend a small FOV at flyby, so only a few steps will be required to scan across the asteroid. At the start position of the scan mirror field of regard, the instrument is viewing the solar-illuminated calibration plaque.

Optical Design

The NIS optics consist of a scan mirror, an aperture stop, a telescope mirror, and a Rowland circle spectrometer, which uses the first and second orders from the diffraction grating. Figure 2 shows the optical layout of the NIS.

The scan mirror rotates to provide a 140° field of regard. Between the scan mirror and the imaging mirror is a 20 × 25 mm rectangular aperture stop that provides adequate sensitivity. The location of this stop between the mirrors was selected to minimize the sizes of the scan and imaging mirrors. Fig. 2b shows the elliptical area of the mirror used when the FOV is at an extreme angle. This area varies with the FOV direction and is a minimum when the FOV is directed to the end of scan.

Imaging is performed by a single off-axis parabolic mirror that images the scene at the field stop, the entrance slit of the spectrometer. This mirror has a focal length of 75 mm, and its center is 22.5 mm off-axis. The mirror provides adequate image quality over the small FOV. It images the scene at the field stop with a scale of 0.76°/mm. The field stop is either of two selectable slits: a movable narrow slit with dimensions of 1 × 0.5 mm giving a spatial FOV of 0.76 × 0.38° or a fixed 1-mm square slit with an FOV of 0.76° square. A shutter allows the field stop to be closed for recording dark signals. The imaging mirror also images the aperture stop at the diffraction grating. This ensures that the grating has the minimum size and is evenly illuminated.

The NIS operates from 800 to 2600 nm by using first and second spectral orders of the grating. The two ranges are 800–1500 and 1300–2600 nm. These orders are separated by a dichroic beamsplitter that has high transmission above 1550 nm and high reflectance below 1450 nm as shown in Fig. 3. The long wavelengths are transmitted to the InGaAs detector and the short ones are reflected to the Ge detector. The NIS has two

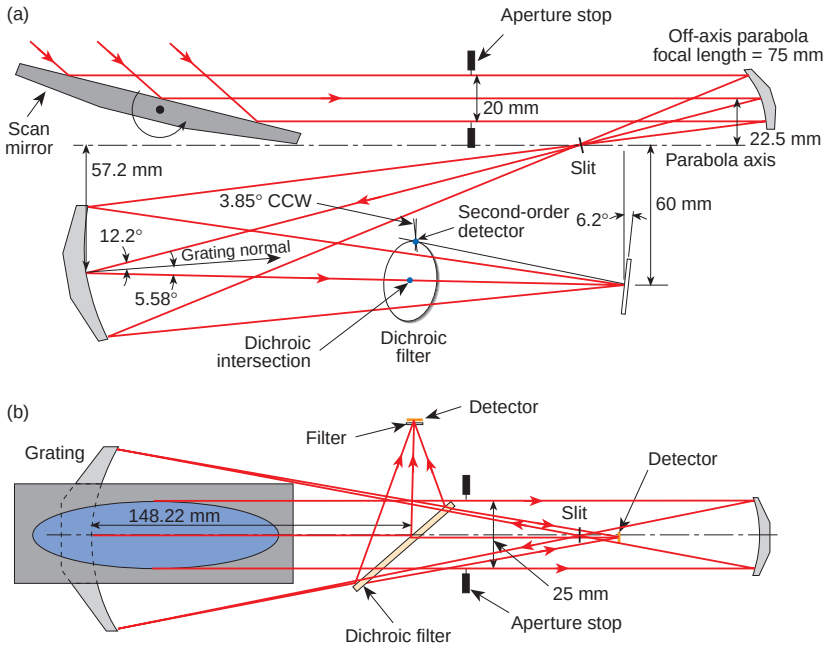

Figure 2. Optical schematic of the NIS. (a) Side view. (b) Top view. (CCW = counterclockwise.)

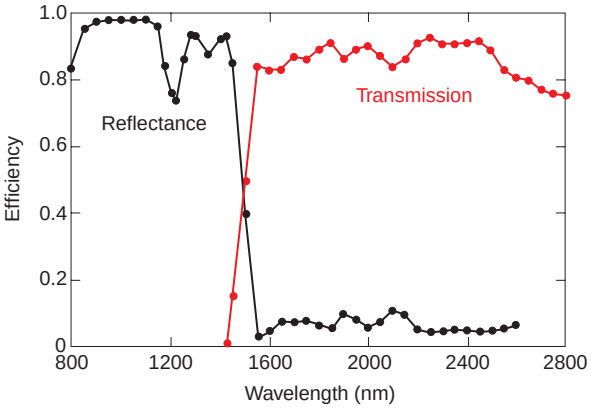

Figure 3. Reflectance and transmission characteristics of the NIS dichroic beamsplitter.

one-dimensional image planes, each 1 × 16 mm. The detector arrays have 32 elements; each element is 1 mm high by 0.5 mm wide, corresponding to the image of the slit with a magnification of unity.

The diffraction grating operates in the Rowland configuration, i.e., it both disperses and re-images the energy. It has a radius of curvature of 200 mm and a ruling of 57 grooves/mm. These measurements combine to produce a spectrum that has a dispersion of 88 nm/mm in the first order. The traditional problem with a Rowland circle spectrometer is astigmatism, which is reduced by making the grating toroidal. The grating radius of curvature in the direction perpendicular to the dispersion direction is 193.7 mm. This radius cancels the astigmatism at the center of the spectrum although it is still present at the extreme wavelengths. Reduced astigmatism allows adequate spatial resolution in both the spectral and spatial directions. It also concentrates the energy on the detector.

The diffraction grating and mirrors have reflecting surfaces of gold that provide optimum reflectance for the spectral range above 800 nm.

Spectral Crosstalk

Second and higher order, shorter wavelengths are prevented from reaching the InGaAs detector by the dichroic beamsplitter, which has transmission of less than 0.1% for wavelengths below 1300 nm. Higher spectral orders at the Ge detector are eliminated by a two-zone filter located close to the surface of the Ge detector. One zone attenuates light below 770 nm and is effective for channels at wavelengths below 1150 nm (1.5 × 770 nm), and the second zone attenuates light below 1000 nm falling on channels above 1150 nm. The boundary between the two zones, centered at 1.12 μm, causes a 40% loss of light that is confined to a single channel.

Because of the finite reflectance of the dichroic filter and nonzero response of the Ge detector for first-order wavelengths above 1600 nm, some spectral crosstalk from the first-order to the second-order detector is expected. The crosstalk has been measured and analyzed, and small correction factors will be applied to the signals from the first four Ge elements.

In-flight Calibration

For in-flight calibration, a diffuse gold plaque is located at the scanner end of the instrument where it extends beyond the edge of the aft deck and intercepts direct sunlight. The plaque is made with Infragold LF (trademarked), which is a porous metal surface with a gold coating. This material was selected for its acceptable spectral range, stability over time, and reasonably low specular reflection. The viewing (emission) angle of the plaque by the NIS optics is fixed at 75°.

Stray Light

The NIS is designed to minimize the entry of stray light into the focal plane. Both the scan and telescope mirrors have very low scatter surfaces. Baffling along the light path prevents stray reflections from reaching the focal plane; no direct light path exists from the scene to the imaging mirror; and a zero-order trap prevents reflection of stray energy. Of more concern is light scattering from one part of the spectrum to another, which depends on the quality of the grating.

DETECTORS

Detector Arrays

The spectral response curves of the Ge and InGaAs detectors are shown in Fig. 4. The Ge detector is a

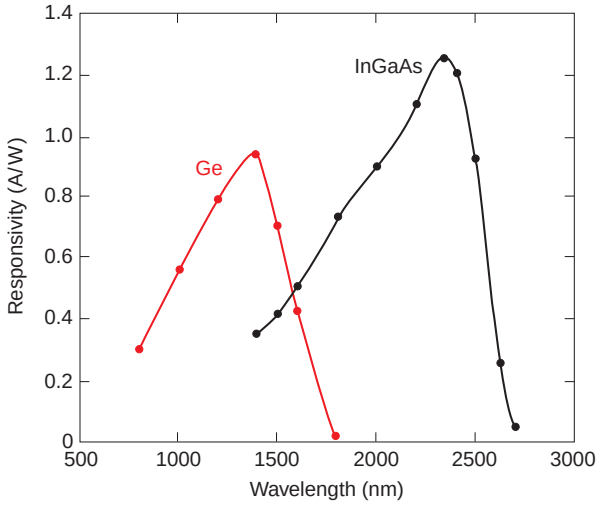

Figure 4. Spectral responsivity of Ge and InGaAs detectors.

32-element, commercially available, photodiode array, which was purchased from EG&G Judson for the shorter wavelength detector. For the longer wavelengths, the InGaAs detector was obtained from Sensors Unlimited, Inc. The InGaAs array is formulated with a suitable long-wavelength cutoff of 2600 nm. This array is the same size as the Ge array and was made by paralleling groups of 10 of an existing 50-μm-wide photodiode array design and increasing the height from 0.25 to 1 mm. Obtaining consistently good performance is difficult for this very large size InGaAs detector.

Detector Electronics

Figure 5 shows a simplified schematic with information applicable to both detector electronics packages. Each detector element has a dedicated transimpedance preamplifier that incorporates a low-pass filter. Each element acts as a separate photodiode with a common cathode for all 32 diodes in each array. A switch multiplexes the outputs of the 32 preamplifiers to a single analog-to-digital (A/D) converter. This conversion is fast in comparison with the response time, so a very simple system can be used. The same converter also digitizes several temperatures in each unit. Each detector assembly functions independently, and both are controlled and powered by the DPU. Data are obtained once per second from both detectors. Design constraints included low power consumption, passive cooling, radiation tolerance, operation in vacuum, and robust compact mechanical design. The detectors require a preamplifier circuit that provides high current sensitivity, but low bandwidth.

Variations in diode resistance also cause the noise gain to vary, resulting in an output voltage shift with no light on the photodiode—a zero or dark drift. Drifts in the amplifier offset with temperature or time also cause a dark drift. To correct for any drifts, frequent dark measurements, taken with the shutter in front of the slit, are used to record the dark background.

The relatively high shunt resistance of the Ge detector led to the selection of an operational amplifier using a field-effect-transistor input, the AD648. A selectable ×10 voltage-gain stage was added before the 12-bit converter to allow for increased sensitivity on weak signals, since the preamplifier noise was low.

For the InGaAs amplifier design, the very low detector shunt resistance means that the transimpedance amplifier will be operating at very high noise gain. Therefore, an operational amplifier with very high open-loop gain and low-voltage noise is needed, as well as low-offset voltage and drift. These requirements are in addition to low current noise, bias current, and power and high-radiation tolerance.

Because low-offset voltage was crucial, single packaged operational amplifiers were used, and, after a broad selection process, the OP97A was chosen. The OP97A is a bias-compensated bipolar operational amplifier that has good noise specifications and has proved to be successful. A significant dark offset, larger than the signal, is present, which is measured as often as needed, in the minutes or hours range, and then subtracted in data processing on the ground.

Because the shunt resistance of the photodiode nominally doubles for each 8°C reduction in temperature, cooling greatly improves the performance.

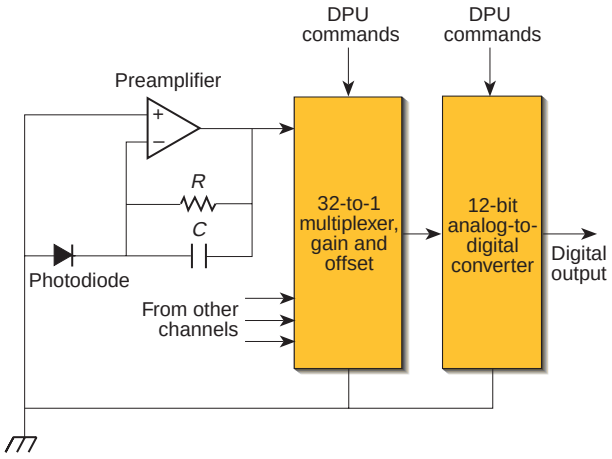

Figure 5. Block diagram of detector electronics. Each channel has a dedicated transimpedance amplifier with low-pass filtering. A multiplexer sequentially connects each of the 32 preamplifier outputs to the analog-to-digital converter. For the Ge detector only, a selectable gain amplifier is located between the multiplexer and the digitizer, with a gain of either 1× or 10×. *R* = resistance; *C* = capacitance. *R* is 200 MΩ for Ge channels 1 to 22; 500 MΩ for Ge channels 23 to 32; and 100 MΩ for all InGaAs channels.

MECHANICAL DESIGN

The structure is built out of aluminum in two sections. The scanner section contains the scan motor and scan mirror and supports the calibration plaque. The telescope section contains the primary mirror, slits and shutter, grating, dichroic beamsplitter, and detector mounting flanges. All the reflective optics are manufactured on aluminum substrates. The combination of aluminum optics and aluminum structure provides for an optical system with minimal sensitivity to bulk temperature change.

Scanner, Slits, and Shutter

The line of sight is positioned by rotating the scan mirror with a four-phase stepper motor. This motor rotates 15° per step and is coupled to the scan mirror through a 75:1 reduction gear providing 0.2° of rotation per step. Reflection off the scan mirror doubles the

step size of the line of sight to 0.4° per step. At launch, the mirror is stowed parallel to the cover and held securely in place by the cover. The "nadir" and the "start" positions of the scan mirror are detected by two light-emitting diodes that shine through slots in a vane rotating with the axle of the scan mirror. The light from the light-emitting diodes is transmitted through the slot in the vane and captured by a fiber-optic cable connected to a sensor at the support electronics.

Three identical motors operate the scan mirror, slit, and shutter. Only one phase of a motor is excited at any time. Each stepper motor also has both primary and secondary windings, providing backup in case of failure of the motor windings.

The wide slit is fixed in position within the slit assembly. The narrow slit is mounted to a lever arm that can be rotated to move the narrow slit in and out of the optical path. After it reaches position, the slit is held in place magnetically with no further power required.

The shutter is also a motor-operated lever arm within the slit assembly, but with no opening in it. Because it is a single point of failure, the lever arm is equipped with a return spring to open the shutter when power is removed. To hold the shutter closed, therefore, the stepper motor must be continuously energized.

To match the orientation of the NIS field of regard to the desired orientation for NEAR, the instrument is mounted on a magnesium bracket at 45° to the aft deck of the spacecraft. Epoxy–glass spacers provide a high degree of thermal isolation between the aft deck and the instrument.

Cover

The cover is designed to be opened one time only in space. Before it is opened, the cover helps to maintain cleanliness of the optics, hold the scan mirror in place during launch, and add to the structural strength of the housing during launch by providing structure across the large mirror opening. The spring-mounted cover is held closed at launch with a pin that is pulled out of the latch by either of two redundant pyros, allowing the cover to open. Microswitches indicate the closed/fully open condition.

THERMAL DESIGN

The NEAR mission configuration ensures that the solar arrays and high-gain antenna always point within 30° of the Sun so the instruments mounted on the aft deck are always in the shadow of the spacecraft. This configuration provides an excellent opportunity to improve detector performance by passive cooling to –35°C by radiation to space. Thermal gradients within the optics structure should be held to less than 10°C. Maintaining this temperature must be accomplished while the NIS is attached by the bracket to the aft deck, which may be at temperatures as high as +40°C or as low as –30°C.

The most stressing case is when the aft deck is at maximum temperature. The design allows progressively decreasing temperatures from the aft deck to the detectors, with thermal isolation, radiative cooling, and operational heaters controlling the distribution of thermal gradients. The largest temperature drop is across the thermal isolators that are used to attach the bracket to the aft deck, and a relatively low thermal gradient occurs throughout the bracket structure. The NIS is bolted to the bracket through two titanium flexures, which we call the NIS feet. Because of the low thermal conductivity of titanium, a high thermal gradient can be maintained across the feet. Operational heaters keep the NIS optics at about –10 to –15°C. The detector assemblies are bolted to the optics housing through thermal isolators to minimize heat transfer from the housing to the detector assemblies. The backs of the detector housings are large radiators that provide cooling for the detectors and detector electronics. The balance of detector electronics power dissipation and radiator cooling results in operating temperatures of about –30 and –40°C for the Ge and InGaAs detectors, respectively, and just slightly warmer for the detector electronics boards. No operational heaters are required for the detectors. Survival heaters keep temperatures at around –40°C during the cruise phase when the instrument is turned off. To minimize heat loss and, hence, the survival heater power, the cover is kept closed until after aphelion.

DATA PROCESSING UNIT

The NIS/Magnetometer DPU controls the NIS and the Magnetometer. The DPU interfaces to the spacecraft command and telemetry processor (CTP) over the redundant MIL-STD-1553 databus and provides power conditioning, digital control, and data readout for both instruments.

The DPU software handles uplinked commands, collects NIS data, and sends telemetry data to the CTP. Commands for configuring the NIS mechanisms include manual positioning of the mirror, shutter, and slit; selecting primary or backup motor windings; and selecting 15- or 20-V motor operation. The DPU contains the software and performs the commands; the support electronics provide the motor driver and fiducial monitoring electronics.

NIS data acquisition sequences integrate a specified number of spectra, telemeter the result, and move the mirror a specified amount. The process is repeated a number of times, as specified in the sequence.

Spectra sent to the CTP are usually placed on a solid-state recorder for later downlink, but they can also be sent directly to the ground. Housekeeping data, temperatures, currents, mechanism status, and sequence information are also transmitted with each set of spectra.

The NIS does not perform any data compression before sending data to the ground, but it can sum up to 16 frames of data onboard.

PRE-FLIGHT CALIBRATION AND CHARACTERIZATION

Overview and Facilities

The NIS was thoroughly calibrated at the individual component level and as an integrated instrument before launch; further in-flight calibrations are also being performed.

Instrument-level calibration tests were performed in the Optical Calibration Facility of APL. In this facility, the instrument is mounted on a motion stage inside a vacuum chamber with an internal diameter of 1.3 m and a length of 2.0 m. The motion stage can rotate the instrument in azimuth and elevation. The interior of the vacuum chamber is surrounded by a cold wall through which an external refrigerator circulates a cooling fluid to reduce the internal temperature to as low as –40°C.

The instrument can be turned to view either a field- and aperture-filling, extended source outside the chamber window or a collimated beam from a point source or from the exit slit of a monochromator.

Dark Signals and Expected SNR

Extensive prelaunch testing was conducted in thermal vacuum conditions to measure the detector dark signals and the noise in the measurements. Such tests are necessary to correct for detector drift and establish a basis for SNR predictions. In-flight dark data are now available and are used for dark signals and SNR predictions in this article. The prelaunch data were very similar to the in-flight data obtained to date.

The in-flight dark signal levels of the Ge detectors show the intentional offset of about 80 A/D converter data numbers (DNs), with very little variation between channels for unity gain and only a ±2 DN variation for gain 10. The 80-DN offset is deliberately introduced in the electronics to ensure that any electronics drift or offset changes that occur during 4 years in flight will not result in dark signals of less than zero volts, which could not be measured by the digitizer. The InGaAs channels have a "baseline" intentional offset of about 1000 DNs. Several channels differ significantly from this baseline offset owing to preamplifier offsets that add to the intentional offset. The significant preamplifier offsets are a direct result of the low shunt resistance of the InGaAs photodiodes.

Figure 6 shows the calculated signals and SNRs for the initial flyby of Eros. The signal levels in the InGaAs band are low, so the high offsets should not saturate any channels. The large change in predicted DN for the last 10 Ge channels is due to the larger feedback resistors used for those channels. The SNR data are calculated for a 10-s observation, which includes 4 s of dark data and 2 s of unused time for slit changes. Longer times are possible for the flyby, but this time is consistent with the amount of time available during low-altitude orbital operations. The ultimate accuracy of these data will be limited by calibration, rather than SNR, since the SNR is so high.

Spectral Calibration

Spectral calibration was performed by imaging the filament of a stable (but uncalibrated) incandescent source onto the entrance slit of the monochromator whose exit slit was at the focus of the collimator. The signals from the detector arrays were recorded as the monochromator wavelength was stepped in 5-nm increments over the second-order wavelength range (Ge detector) and 10-nm increments over the first-order wavelength range (InGaAs detector). The spectral calibration was based on locating the 50% response points for each element.

The average results for three data sets collected at different temperatures are shown in Fig. 7. The Ge spectral calibration is given by

$$\lambda(\text{nm}) = 794.6 + 21.61n \qquad (1)$$

in which n is the element number between 1 and 32. The accuracy of this equation for the three data sets is approximately ±0.5 nm.

For the InGaAs elements the center wavelength is given by

$$\lambda(\text{nm}) = 43.11n - 50.8 \qquad (2)$$

in which n is the element number between 33 and 64. The accuracy of this equation for the three tests is approximately ±3.5 nm. The error is primarily a systematic error between tests performed at different temperatures.

The full spectral range of the Ge array is 805.4 to 1497 nm, and the full range of the InGaAs array is 1307 to 2730 nm; however, these ranges are further limited by the falling responses of the InGaAs detector at the long wavelengths and the efficiency range of the dichroic filter. Spectral calibrations of the wide slit show that the average offset of the wide slit spectrum relative

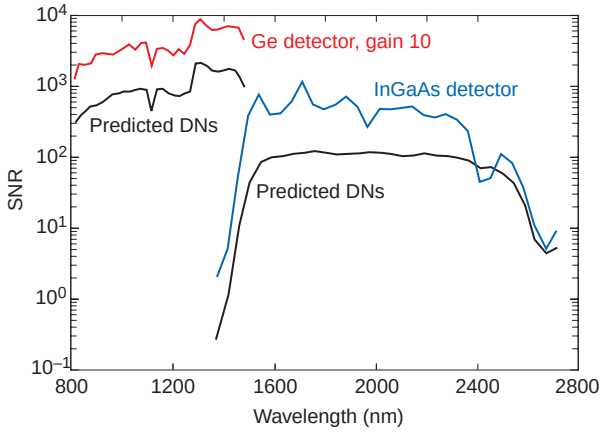

Figure 6. Predicted NIS data number (DN) levels and signal-to-noise ratios (SNRs) for the low-phase-angle flyby observations of Eros. Signal levels were estimated using nominal values for solar flux, the reflectance of Eros, heliocentric distance (D = 1.75 AU), the phase angle at the time of the flyby ($\alpha = 0°$), and radiometric calibration constants determined from pre-flight calibrations. The noise was estimated using in-flight dark signal measurements obtained on 21 May 1996. The assumed spectrum acquisition sequence uses the narrow slit over a 10-s interval (4 s for Eros data, 2 s for shutter changes, and 4 s for dark data).

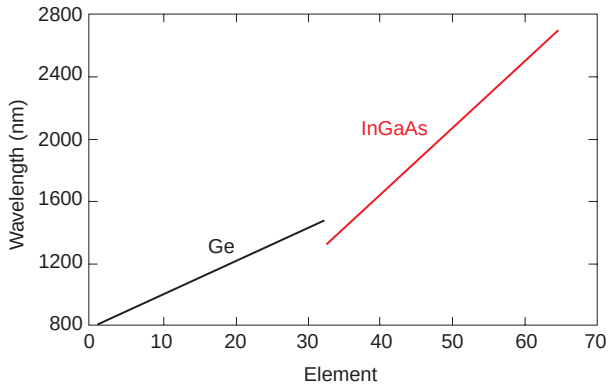

Figure 7. Spectral calibration data and linear regression.

to the narrow slit is –3.3 nm for the Ge detector and twice this for the InGaAs detector, which corresponds to a linear offset of 0.075 mm between the slit centers.

Radiometric Calibration

The radiometric response of the NIS was determined in a number of tests by recording the response while viewing a calibrated field- and aperture-filling integrating sphere. The radiometric response of the NIS to a radiance source is shown in Fig. 8. The Ge data show the loss of signal at 1125 nm, caused by the boundary between the two zones of the filter, and higher response above 1290 nm because of higher amplifier gain. The nominal ratio between the signals from the two slits is 2; however, the average is measured to be 2.1 with unexpected variations from element to element of as much as 10%.

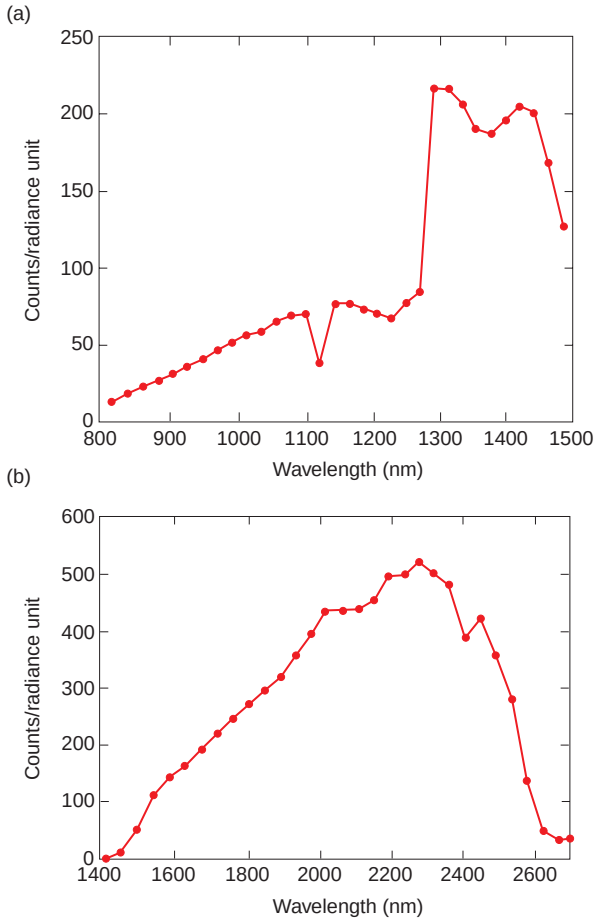

Figure 8. Radiometric calibration of the NIS for (a) Ge and (b) InGaAs detectors. (Radiance unit = mW · cm^{-2} · sr^{-1} · μm^{-1}.)

The reflectivity of the scan mirror, and therefore the radiometric calibration, is expected to change with scan angle since the angle of incidence is changing. This effect was also measured during the testing.

Instrument Characterization

Several other tests were made to measure the performance of the NIS. Its sensitivity to polarized light was measured by taking measurements with and without a polarizer in the beam. The scan mirror, the grating, and the dichroic filter are all polarization-sensitive components. The instrument was found to introduce as much as 10% polarization into the incident light. For the expected very low polarization levels from Eros, the effect will be insignificant, because a source that is linearly polarized with 10% polarization in the most unfavorable orientation will change the signal by only 0.5%.

The off-axis response of the NIS was measured to examine its response to out-of-field light. It was found that energy from a source only 1° from the center of the slit is reduced by 4 orders of magnitude.

Each detector array is aligned independently for focus, position, and angular orientation. For efficient energy collection, the entrance slit must be imaged squarely onto each array, and for each array to see the same target area, the two arrays must be co-aligned. Tests showed the arrays are spatially aligned to an acceptable accuracy of about 0.01° or a position of 0.014 mm.

Co-alignment with Other Instruments

Reference optical cubes on the Multispectral Imager (MSI), the NIS, and the NEAR Laser Rangefinder (NLR) were used to measure the alignment of the instruments relative to each other and to an alignment cube on the spacecraft. Figure 9 shows the alignment of the MSI FOV, the NLR transmitter, and the NIS for a range of mirror steps from 70 to 80 relative to the spacecraft's x' axis.

The scan mirror movement, which shifts the line of sight nominally by 0.4° per step, was also calibrated. A repeatable and acceptable error of 0.75 of a step was found to build up over the full scan range.

Measurements of Geologic Materials

As part of the pre-flight calibration and characterization of the NIS, spectra of more than 30 rock, mineral powder, meteorite, and other samples were measured while the instrument was in vacuum and at nominal operating temperatures. This was accomplished by locating the samples at the focus of the collimator so they could be imaged by the NIS. The samples were illuminated with a quartz halogen lamp and measured using all combinations of slit width and gain states.

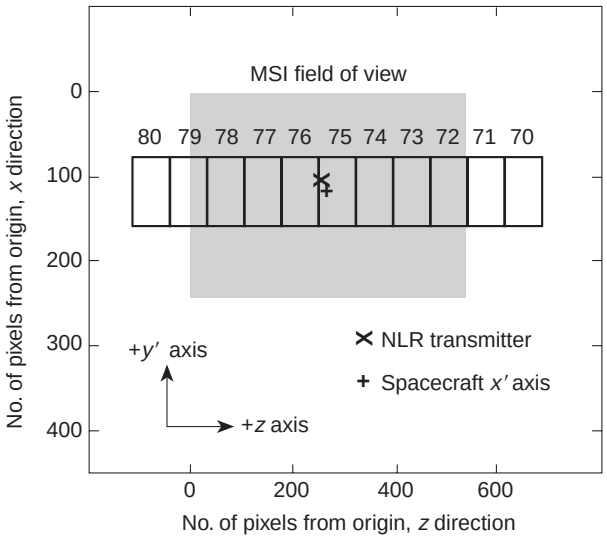

Figure 9. On the x' axis, the spot formed by the NLR transmitter and the NIS FOV through the narrow slit for different mirror positions shown in MSI pixel coordinates. (The corresponding step number is written beside each NIS FOV shown.)

Examples of some representative NIS spectra of these materials, calibrated relative to a Halon standard also observed by the NIS, are presented in Fig. 10. The spectra are completely consistent with previous spectra of these materials and demonstrate the spectral resolution and fidelity that can be achieved by the NIS. Some of these samples were also measured using the multispectral filters of the MSI during its pre-flight calibration period, and Fig. 10 indicates that the agreement between NIS and MSI spectra for the region of spectral overlap (900 to 1050 nm) is excellent. The sample spectra also serve as a useful database for development and refinement of data reduction and analysis algorithms before the collection of actual Eros spectra in 1999.

PRELIMINARY MISSION PLANNING

In-flight Calibration

In-flight calibrations of the NIS will monitor and measure the following: (1) the instrumental dark current and its variations with time and temperature, (2) the radiometric calibration coefficients needed to convert instrument DNs into flux units, (3) the effects of stray and scattered light in the instrument, and (4) the spatial and spectral alignment of the Ge and InGaAs detectors.

Radiometric calibration checks will be achieved primarily from observations of the onboard diffuse gold calibration plaque after the cover is opened. The calibration plaque will be measured frequently in flight by orienting the spacecraft to a geometry that allows sunlight to be reflected off the calibration plaque and into the instrument. During the Earth–Moon flyby in January 1998, additional calibration measurements of the Earth and Moon were scheduled to verify instrument health and wavelength calibration (by observing terrestrial H_2O absorption features) as well as to provide an independent assessment of the NIS radiometric calibration through observations of well-characterized lunar surface regions.

Plans at Eros

NIS observations of Eros will be coordinated with MSI imaging observations to realize fully the synergy between these two instruments. Observation sequences will usually be designed so that full NIS spectral coverage is obtained for each MSI FOV.

Each NIS spectrum will be tagged with pertinent instrumental and spacecraft housekeeping data as well as observation geometry information (e.g., latitude, longitude, and incidence and emission angles). This information will allow each NIS spectrum to be

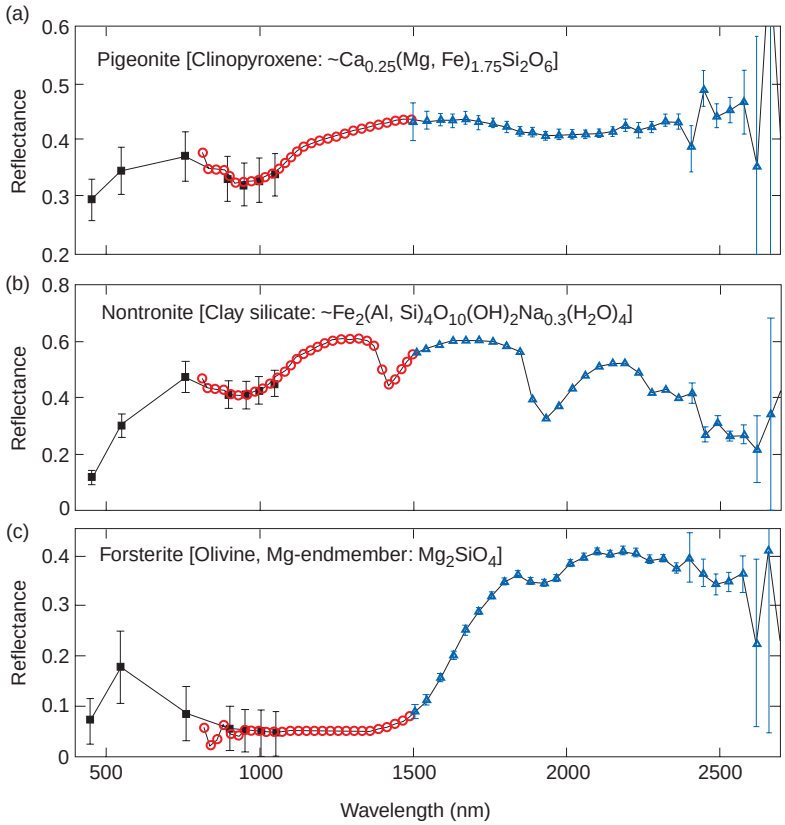

Figure 10. Spectra of typical mineral and rock samples measured by the NIS during pre-flight calibrations at APL. Data from the Ge detector are shown as circles; data from InGaAs are triangles. Shown for comparison are the seven-color spectra of these same samples as measured by the MSI instrument and plotted as squares with error bars. Both the NIS and MSI measurements were calibrated through observations of the same Halon reflectance standard. These plots thus show how well the two instruments agree in the region of spectral overlap. Error bars in MSI spectra include variance due both to noise in the data and to shadows in the images of the samples. (a) Spectrum of pigeonite powder HS199. The diagnostic 1000- and 2000-nm pyroxene absorption bands are clearly detected. (b) Spectrum of nontronite powder SWa-1.a. Narrow spectral features near 1400 and 1900 nm are caused by adsorbed and structural water within this clay mineral. (c) Spectrum of forsterite fragments GDS70.c. The strong olivine absorption feature centered near 1200 nm dominates this spectrum. All samples were kindly provided by Roger Clark of the U.S. Geological Survey.

mapped onto the surface of Eros in near–real time so that the science team can keep track of which regions have been covered. The long time in orbit will result in a global map showing the distribution of minerals across the surface of Eros.

The expected signal levels are low enough that the gain 10 state of the Ge detector should be used for most data. During the Earth flyby and late in the mission, the heliocentric distance is reduced, and use of the unity gain state may be required to avoid saturation. The wide slit can be used to improve SNR at the expense of spectral and spatial resolution. Because predictions that show good SNR should be obtained with the narrow slit in most circumstances (through adding of multiple spectra), the narrow slit is expected to be used for most observations. Dark data will be obtained frequently. Although exact observing plans have not been defined, it is planned to interleave dark data with spectra of Eros—the time between dark data is expected to be measured in seconds rather than minutes.

The calibrated data from Eros will be archived and distributed to the NASA Planetary Data System, and much of it will be rapidly available on-line for downloading by anyone via the Internet and World Wide Web. The data will be used by the science team as well as asteroid scientists worldwide to investigate fundamental questions about the nature of asteroid surfaces as well as the link between asteroids and meteorites. The data are relevant to the following specific science activities:

- Studying surface mineralogic variations associated with impact craters as a way to probe the interior of Eros
- Examining the spectra of fresh craters and steep walls or slopes as a way to assess the role of putative "space weathering" processes in the alteration of asteroidal surfaces
- Providing clues to the origin and geophysical structure of Eros by searching for evidence of large-scale mineralogic variability and coherent spectral units
- Constraining models of the origin and evolution of ordinary chondrites and other meteorites by comparing the detailed mineralogy and chemical composition of a typical S-type asteroid with the major meteorite families

Many more issues will be addressed by the NIS data, and many surprises are likely to occur from this first-ever close-up examination of a primitive body. By providing high-quality global mineralogic information about the surface of an asteroid, the NIS investigation will play a major role in the continuing exploration of our solar system.

ACKNOWLEDGMENTS: The authors would like to express their thanks to the entire NIS team, whose efforts led to the successful completion of this instrument on a very tight schedule. From concept through launch support and mission operations after launch, the entire team has given exceptional effort to make this instrument and mission a reality. The contributions to this article of Scott Murchie, Jim Bell (Cornell), and Steve Krein (Orbital Sciences Corp.) also are appreciated. This work was supported under contract N00039-95-C-0002 with the U.S. Navy.

THE AUTHORS

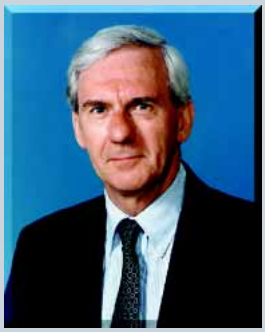

KEITH PEACOCK received a B.Sc. in physics from Durham University in 1961, an M.Sc. in radioactivity from Birmingham University in 1962, a Ph.D. in astronomy from Manchester University in 1967, and an M.S. in technical management from The Johns Hopkins University in 1984. Before coming to APL in 1979, he worked at Bendix Aerospace Systems at the Los Alamos National Laboratory. During his first 8 years at APL, he worked on the Submarine Security Program. He later joined the Space Science Instrumentation Group. Dr. Peacock received two Lawrence Hafstad Fellowships for work on optical design projects in JHU's Department of Physics and Astronomy. His primary field of interest is optics; he designed the five MSX UVISI spectrographs, the Special Sensor Ultraviolet Spectrographic Imager, the Global Ultraviolet Imager, and the Near-Infrared Spectrometer for NEAR. Dr. Peacock also teaches optics at JHU's G.W.C. Whiting School of Engineering. His e-mail address is keith.peacock@jhuapl.edu.

JEFFERY W. WARREN received a B.S. degree in 1982 and an M.S. degree in 1984, both in electrical engineering, from the University of South Carolina. His thesis research evaluated electro-optical measurements of surface charging of insulators in low-frequency electric fields. He joined APL's Electro-Optical Systems Group in 1984. Mr. Warren's primary activities involve development and testing of prototype and experimental electro-optical systems. His e-mail address is jeffery.warren@jhuapl.edu.

EDWARD H. DARLINGTON received a B.Sc. (Hons.) degree from Durham University and a Ph.D. from the Cavendish Laboratory, Cambridge, England, and is a Chartered Engineer. He has worked in electron physics and elemental analysis and also has experience in electron, ion, light, and ultrasound optics. For the last several years, he has been developing optical sensors for space-based instruments. Dr. Darlington is a member of APL's Principal Professional Staff and the Space Science Instrumentation Group. He teaches courses in electronics and optical radiation detectors at JHU's G.W.C. Whiting School of Engineering. His e-mail address is edward.darlington@jhuapl.edu.